DEVELOPMENT OF POWER CONVERTER FOR HIGH POWER PIEZOELECTRIC MOTORS

T. Schulte, N. Fröhleke

Institute of Power Electronics and Electrical Drives
University of Paderborn, FB14/LEA
e-mail: schulte@lea.uni-paderborn.de

Abstract

Several types of piezoelectric motors are known to deliver few watts of mechanical output power. This paper deals with the design and development of a LLCC-resonant converter for a novel type of high power piezoelectric motor of up to 4kW mechanical power being used in avionics. The development of a laboratory power supply became necessary, since suitable power supplies for testing the novel piezoelectric motor during its breadboard stage are not available on the market. The general function of the LLCC-resonant converter which also provides a DC-offset voltage for avoiding depolarisation problems is described, implementation highlights are outlined and the weight distribution is discussed with respect to future development of power converters for avionics.

1. INTRODUCTION

Several types of piezoelectric motors are known, like traveling wave type ultrasonic motor or inchworm motor, etc., see [1]. To the authors best knowledge the most powerful up to date piezoelectric motors deliver about 20 Watt of mechanical output power at maximum efficiency of about 20%.

Within the scope of the EUREKA-project PAMELA (Piezo Active Motor for more ELectrical Aircraft) the development of a high power piezoelectric motor (HPM) is aimed by company SAGEM SA. The HPM is designed for replacing hydraulic actuators for operating secondary flight control surfaces in aircrafts (like flaps, spoilers, trimming etc., see Fig. 1). Since piezoelectric actuators (motors) combine such features as high power and torque (or force) density especially at low speed and low electromagnetic interferences, they are suitable for being used in avionics.

Requirement for power supplies for piezoelectric motors are very different from those for conventional electrical motors, due to higher operating frequencies and capacitive behaviour of the piezoelectric actuators. The novel HPM is designed to generate a mechanical output power of about $4\,\mathrm{kW}$. The total electrical input power is about $18\,\mathrm{kW}$ active power[1] and from 50 to $80\,\mathrm{kVAr}$ capacitive power. This data reflects a new class of piezoelectric actuators. The operating frequency is about $20\,\mathrm{kHz}$ and the motors voltage amplitudes are in a range of up to $540\,\mathrm{V_p}$. Additionally the HPM should be fed with almost unipolar voltages to avoid depolarisation of the piezoelectric ceramic. Therefore a DC-offset voltage must be superimposed on the supplied AC-operating voltage.

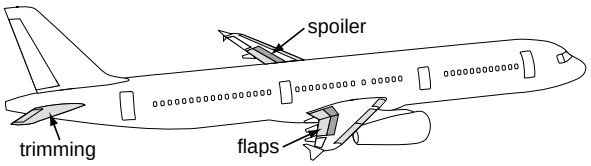

Fig. 1: Secondary Flight Control Surfaces on an aircraft

1. The efficiency of piezoelectric motors is usually less than 25%.

Currently, adequate power supplies are not commercially available. This paper deals with the development of a provisional power supply for testing the HPM under laboratory conditions. In chapter 2 the general operation of LLCC resonant converters is outlined. The realisation problems are discussed in chapter 3, while in chapter 4 the weight distribution for the components is discussed with respect to future development of power converters for use in avionics.

2. LLCC RESONANT CONVERTER WITH DC-OFFSET VOLTAGE

Different types of power converters have been discussed for feeding piezoelectric motors, e. g. [2], [3], [4]. Voltage fed resonant converters with half- or full-bridge topology turned out as most suitable. In [3] LLCC-resonant circuits are proposed for shaping the transfer function so that almost fixed output voltages are generated and in [4] the LLCC-resonant converter is discussed with respect to its advantages in conjunction with a control system.

Fig. 2 shows the general topology (a) (full-bridge) and the frequency response of a LLCC-resonant converter

$$G_{LLCC}(j\omega) = \frac{V_p(j\omega)}{V'_{inv}(j\omega)} = \left[j \cdot \left(\frac{\omega L_s}{R_p} - \frac{1}{\omega^2 L_p C_s} z \right) + \left(1 + \frac{C_p}{C_s} + \frac{L_s}{L_p} - \frac{1}{\omega^2 L_p C_s} - \omega^2 L_s C_p \right) \right]^{-1} . \quad (1)$$

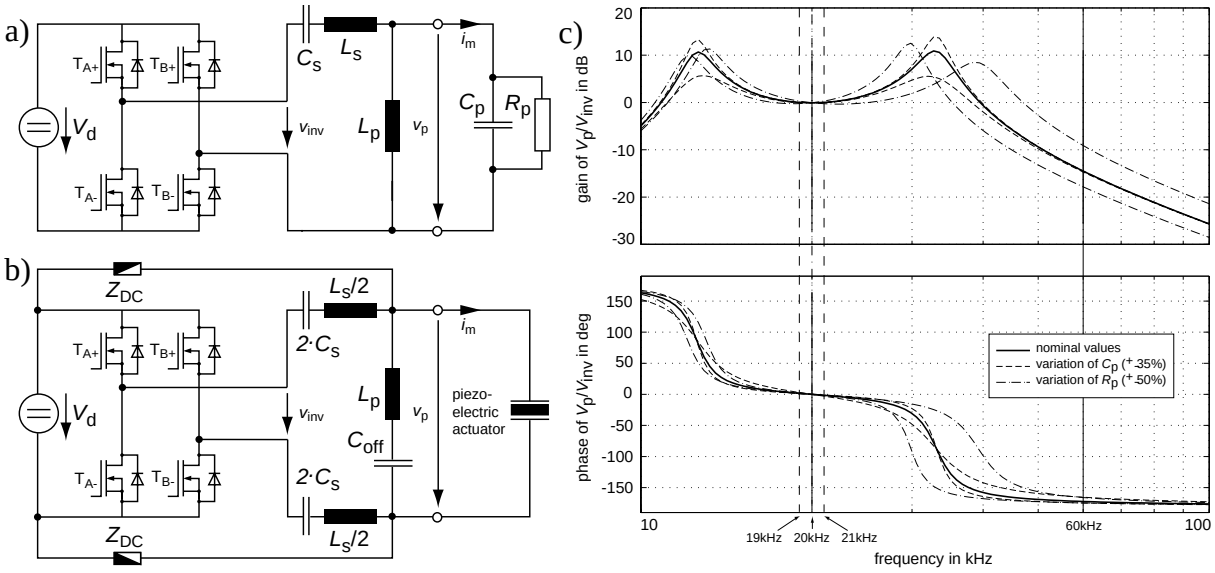

Fig. 2: Topology of a conventional LLCC-resonant converter (a), topology of a LLCC-resonant converter with DC-offset voltage (b) and frequency responses of LLCC resonant tanks (c).

The frequency response of a LLCC-resonant tank designed with $L_p = L_s = 1/(C_{pN} \cdot \omega_{sN}^2)$ and $C_s = C_{pN}$ in Fig. 2c shows a gain of almost 0dB and a phase of almost 0deg around the nominal operating frequency ω_{sN}. C_{pN} is the nominal capacitance of the piezoelectric actuator. Since piezoelectric motors are operated within a relative small bandwidth (20kHz ±1kHz for HPM), the LLCC-resonant technique provides almost impressed motor voltages in a sufficient wide frequency range. In Fig. 2c the load parameters C_p and R_p, representing a simple passive test load, are varied in order to simulate equivalent behaviour of the HPM with temperature (C_p) or load (R_p) variation.

In Chapter 1 it is mentioned, that the motor must be fed with an additional DC-offset voltage. One simple and reliable measure for providing a DC-offset voltage in a range of the AC-voltage amplitude is to use the DC-bus voltage directly linked to the output (see Fig. 2b) via resistors R_{DC} and/or inductors L_{DC} (marked by $\underline{Z}_{DC}$ in Fig. 2b) for decoupling the AC part. The converter stage is decoupled from the DC-offset voltage by series capacitors C_s distributed on both lines of the LLCC-resonant tanks, while additional capacitor C_{off} is blocking the DC-voltage from parallel coil L_p. In order to minimize the influence of the blocking capacitor capacitance C_{off} must by relatively high in comparison to the other components and it must be considered by choosing

$$L_p = \frac{1}{\omega_{sN}^2} \cdot \frac{C_p + C_{off}}{C_p \cdot C_{off}}. \qquad (2)$$

Since only leakage current must be fed to the resonant circuits by the DC link, the realisation of R_{DC} (L_{DC} resp.) is no problem. In the framework of this project resistive decoupling by R_{DC} is used only.

3. POWER CONVERTER FOR HPM

3.1 Topology and Total System

Fig. 4 shows the total topology of the system. The HPM has two times two phases (1a, 1b and 2a, 2b); the phases with index 1 belong to the *main mode* and phases with index 2 belong to the *auxiliary mode*. Each phase of the resonant converter feeds two series connected sets of piezoelectric actuators. The piezoelectric actuators are connected in series in order to decrease the total current. Hence the supply voltage is increased from $270\,V_p$ amplitude (operating voltage of piezoelectric stack) to $540\,V_p$ amplitude.

The AC-voltages of phases with index a and index b of each mode show temporal phase shifts of π, see Fig. 3. The control of the HPM relies on a variation of frequency f_s, temporal phase angle φ_{el} (between 1a and

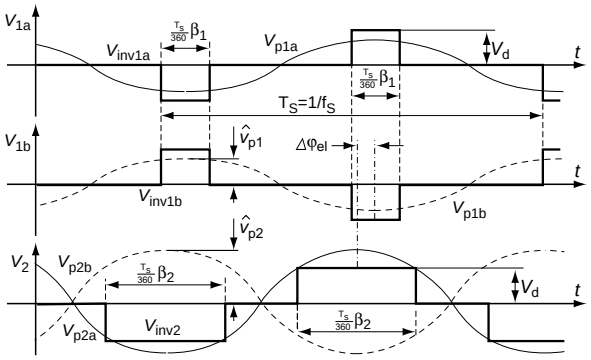

Fig. 3: Principle waveforms of motor and inverter voltages. Due to the behaviour of the LLCC-resonant circuits the fundamental components of the inverters output voltages v_{inv} and corresponding motors voltages v_p are equal.

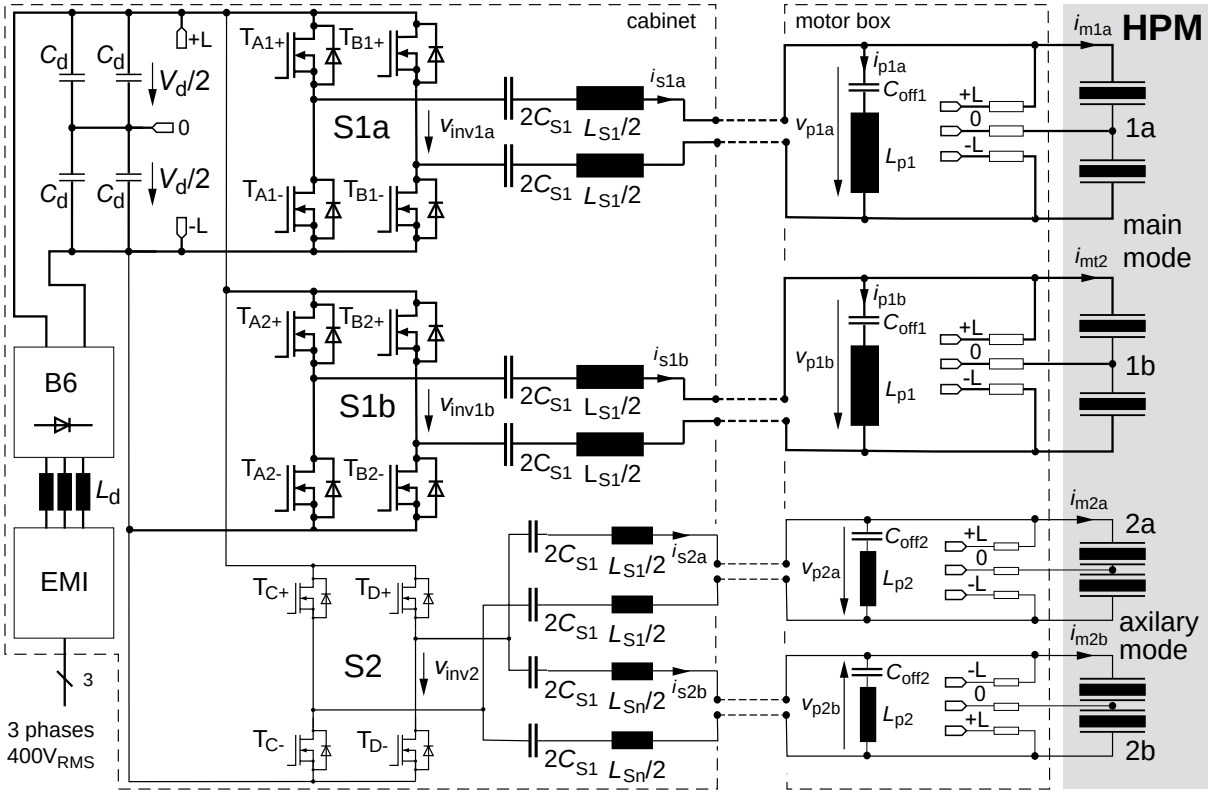

Fig. 4: Topology of two times two phases 80kVAr LLCC-resonant converter

2a, 1b and 2b respectively) and duty cycles β_1 (for 1a and 1b) and β_2 (for 2a and 2b).

Phases 1a and 1b of the main mode are fed by two independent full bridge inverter stages, while phase 2a and 2b of the auxiliary mode are driven by one common inverter stage via two independent resonant circuits, see Fig. 4 and Fig. 5. The DC bus is realized by direct rectification of the 3 phases 400V_{RMS}, 50Hz main[2]. Relative high capacitance value for C_d and input inductors L_d for ensuring a low ripple on the DC bus voltage V_d. Due to the input inductors V_d becomes load dependent and ranges from 520V to 565V. The amplitude of v_{pi} is calculated by

$$\hat{v}_{pi} = V_d \cdot \frac{4}{\pi} \cdot \sin\left(\frac{\beta_i}{2}\right). \qquad (3)$$

Thus, the maximum amplitude $\hat{v}_{pmax} = 4/\pi \cdot V_d$ is about 720V and for limiting the motors voltages v_{pi} β_i must be limited to about $120°$.

Fig. 5 shows the total system including all building blocks. For later implementation of a control system a DSP-board will be used, obtaining the control values like motors speed or amplitude of the mechanical oscillation system, etc. and provides analog control signals for f_s, β_1, β_2 and φ_{el} to the modulator. The modulation signals are transferred to six independent gate driver stages (each driving a half bridge inverter stage) via six independent optical fibres.

The system also contains a *monitoring and control* electronic which monitors the DC bus voltage V_d, the DC bus current I_d, the motor voltages v_{pi} and selected component temperatures.

3.2 Realization of Power Converter for HPM

Fig. 4 shows the cabinet with the main components and in Table 1 the parameters of both phases are listed. The realisation of the auxiliary mode circuit is no problem but of main mode circuit. One problem is the large variation of the load parameters. The active power is varied while different mechanical load is applied to the system. Reactive power is varied since C_p depends on

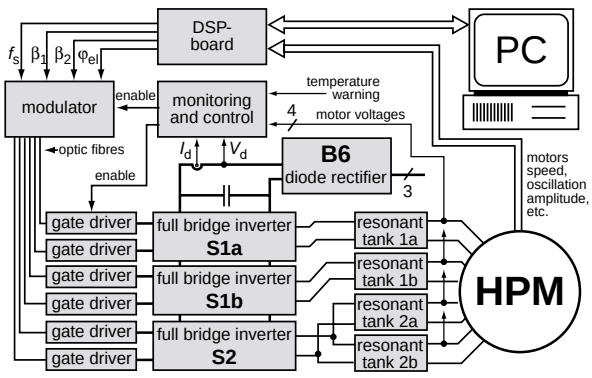

Fig. 5: Building blocks of total system.

2. In aircrafts the main has 3 phases with 115V_{RMS}, 300Hz and heavy voltage and frequency variations.

	phase 1 (each a and b)	phase 2 (each a and b)
P	9kW	160W
C_{pN}	1.75µF	75nF
L_p	38.8µH	908µH
C_s	1.75µF	75nF
L_s	31.7µH	792µH
C_{off}	24µF	1µF

Table 1: Nominal parameters of resonant circuits.

the operating temperature. The HPM is operated in a wide temperature range and therefore the power converter must match a wide variation of C_p (about ±35%). Additionally the operating frequency is varied in a range of ±1kHz . While the frequency response of the system in Fig. 2c shows almost fixed gain and phase values independent from frequency, C_p and R_p, we observe heavy variation of the admittance curves in Fig. 6 (calculated for the main mode with passive C_p - R_p test load).

At the nominal operating point **A** the admittance value is low and the phase angle is $0°$. This means active power feeding by the inverter stage only and a relative low current through the series components C_s and L_s. But in worst case operating points **B** and **C** the admittance values are more than doubled and the phase angle is about $\pm 60°$ implying that high reactive power must be fed by the inverter stage.

Fig. 7 shows simulation results of main mode 1a in operation point **C,** which turned out as worst case with respect to total losses. Corresponding load values calculated from simulation results are stated in Table 2.

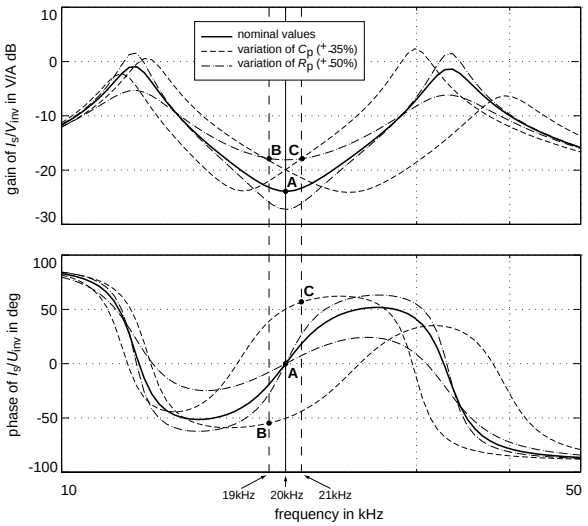

Fig. 6: Admittance curves of LLCC resonant tanks.

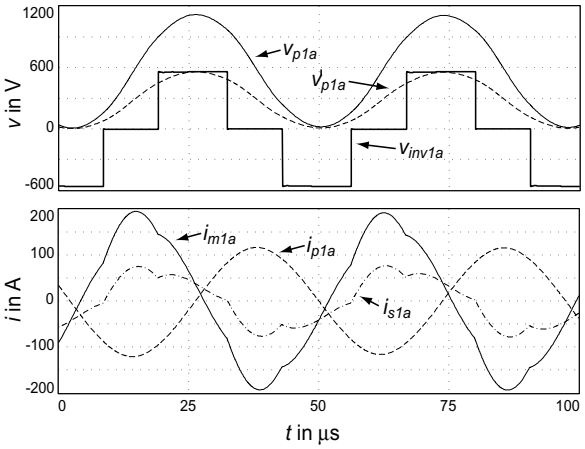

Fig. 7: Simulation of main mode 1a in worst case operation (operation point **C**).

series current $i_{\mathrm{s1a,eff}}$	55.3A
current through parallel coil $i_{\mathrm{p1a,eff}}$	84.0A
motor current $i_{\mathrm{m1a,eff}}$	129.6A
AC motor voltage $v_{\mathrm{p1a,AC,eff}}$	398V
DC motor voltage $v_{\mathrm{p1a,DC}}$	561V

Table 2: Load values of main mode 1a at worst case operation (operation point **C**).

The AC part of the motor voltages v_{p1a} is almost sinussoidal and in phase with the fundamental component of inverter voltage v_{inv1a}. It has $398\mathrm{V_{eff}}$ which results in $563\mathrm{V_p}$ for the AC-amplitude. The DC part is $561\mathrm{V}$ which results in almost unipolar voltage feeding. The total voltage within the system is up to $1100\mathrm{V}$. v'_{p1a} in Fig. 7 represents the voltage for one piezoelectric stack and is almost half of v_{p1a}. While current i_{p1a} is almost sinussoidal (due to sinussoidal v_{p1a}) the motor current i_{m1a} and current i_{s1a} from the inverter stage shows small harmonic distortion.

In summary from above investigation the following points must be taken into account for realization of the provisional power converter for the HPM:

- The design of the highly stressed resonant inductors by high frequencies and currents is difficult. This problem is discussed in more detail in [5].
- Since the inductance values of the main mode are very low (s. Table 1) it is important to ensure that inductivities of cables etc. do not disturb the operation of the LLCC resonant circuits. One measure is to separate the parallel components L_p and C_{off} from the rest of the resonant converter by mounting them close to the HPM in an additional box (called *motor box* in Fig. 4.). The inductivites of cables

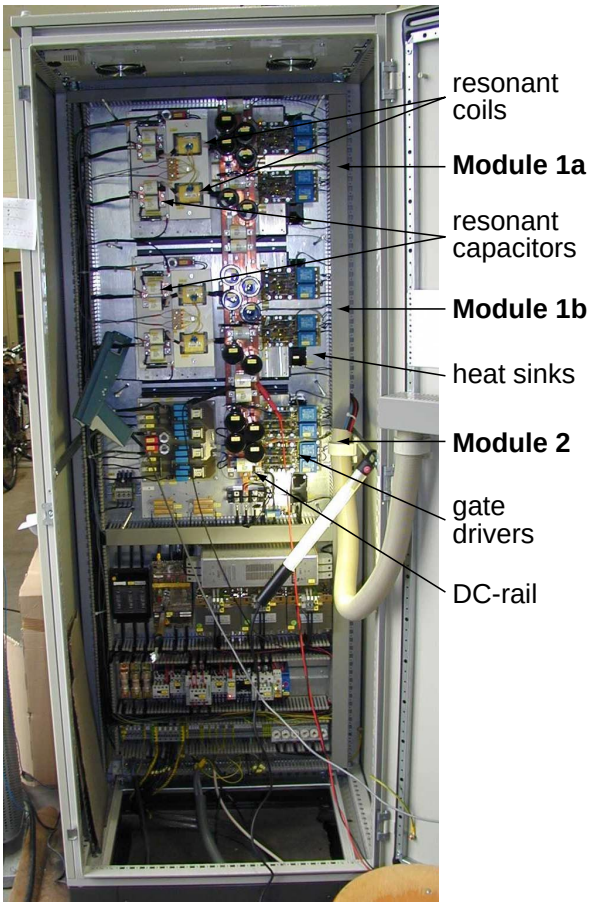

Fig. 8: Cabinet with main components.

between motor box and rest of the converter can be considered when designing L_s.

- Due to the relative high voltages the insulation capability of components, cables, structure, etc. must be considered carefully.
- Semiconductors (half bridge modules) must be oversized with respect to the nominal current due to the unusual operating conditions and the resulting heat dissipation.
- Cables must be oversized due to skin effect at operating frequency of about 20kHz.

Fig. 8 depicts the cabinet of the provisional power converter except components mounted in the motor box. In the upper part of the cabinet the three inverter stages with resonant tanks and heat sinks (called modules 1a, 1b, 2) and the DC-bus are installed, while in the lower part components like EMI-filter input inductors relais, etc. are located.

3.3 Measuring results

First measurements are performed by use of a R_p-C_p-test load (without HPM). Fig. 9a shows a measurement with applied DC-voltage. Therefore C_p-test load can

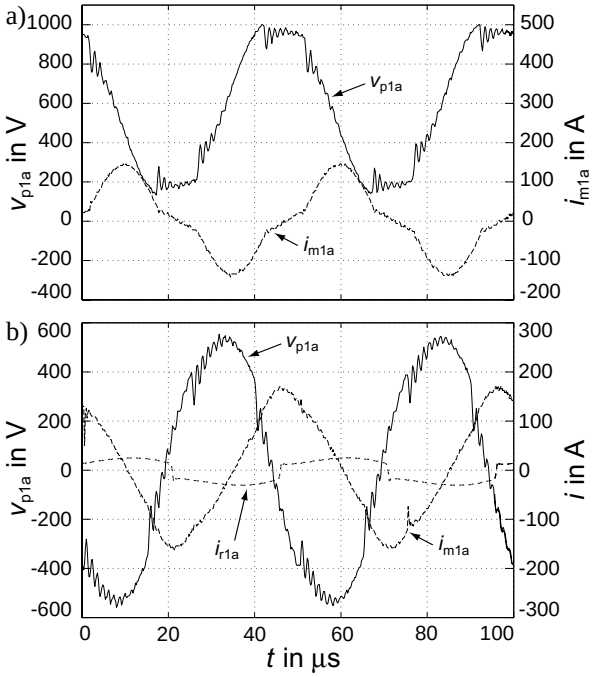

Fig. 9: Measuring results.

be used, only. Since there is no transformer in the system the output voltages are not independent and can only be determined by subtraction of measuring signals from two probes. The maximum permittable voltage for the probes is 1000V. Thus, the AC-amplitude must not be higher than about $440\mathrm{V_p}$. The voltage waveforms shows relatively heavy distortion from sinussoidal waveform. This distortions can not be observed when measuring the voltage by means of a special independent scope. Hence, it results from the measuring method and common mode disturbances.

Fig. 9b shows a measurement without applied DC-voltage. Now the full AC-amplitude for v_{p1a} of $540\mathrm{V_p}$ is driven and load resistor R_p is introduced. Since no low inductive resistor (R_p = 16.2Ω, P = 9kW) was available an additional rectifier is introduced. Due to the inherent inductance of the resistor the waveform of current i_{r1a} measured at the rectifier before R_p is more rectangular than sinussoidal.

4. WEIGHT DISTRIBUTION

As mentioned above the power converter realised in this project is of provisional nature and all components are mounted in the cabinet (and the additional motor box) without considering any weight minimisation. When designing a converter for use in aircrafts the total weight must be reduced significantly.

Fig. 10 (left) shows the weight distribution for all major components of the realised power converter. The total weight is about 41kg. Predominant contributors are the cooling (due to heavy heat sinks) the resonant circuits (due to large inductors) and the DC-bus (due to high capacitance for ripple free bus voltage).

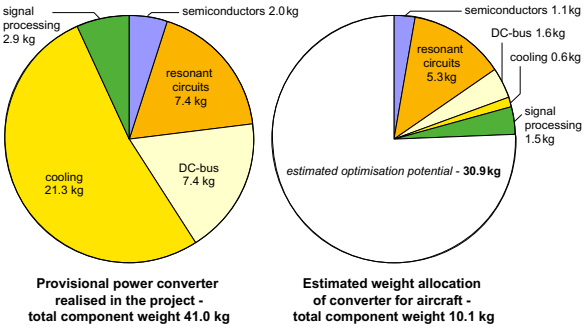

Fig. 10:Weight allocation.

Fig. 10 (right) shows the estimated weight distribution for an optimized design of an resonant converter. The weight of the cooling can be reduced significantly, when the structure of the aircraft is used as heat sink. The weight of DC-bus can be reduced, since the mains in aircrafts has 300 Hz and the voltage ripple can be considered by the control system. A small weight reduction is also possible for the signal processing and semiconductors, etc. but the weight of the resonant circuits can hardly be reduced due to the necessary heavy inductors. The resulting estimated total weight amounts to approximately 10 kg .
Other converter concepts will be taken into account in order to reduce the 10 kg for applications in avionics.

5. CONCLUSION

This paper deals with the development of a LLCC-resonant converter for high power piezoelectric motors. The general concept, the topology and realisation problems are outlined. Simulation and measurement results are presented. The weight allocation is discussed, also stating some key questions governing future developments of low weight power converters for aircrafts.
Commissioning of the power converter in conjuction with the HPM will be performed soon.

6. ACKNOWLEDGEMENT

The development of the high power LLCC-resonant converter is a project in cooperation between SAGEM SA (France) and the institute mentioned above in the scope of the EUREKA-project PAMELA which is an European project with partners from industries and universities.

7. REFERENCES

[1] Sashida, T., and Kenjo, T., “An Introduction to Ultrasonic Motors”, Clarendon Press, Oxford 1993.

[2] Lin, F.-J., Duan, R.-Y., and Yu, J.-C., “An Ultrasonic Motor Drive Using a Current-Source Parallel-Resonant Inverter with Energy Feedback”, IEEE Transaction on Power Electronics, Vol. 14, No. 1, January 1999, pp. 31-42.

[3] Lin, F.-J., Duan, R.-Y., and Lin, H.-H., “An Ultrasonic Motor Drive Using LLCC Resonant Technique”, Proc. of PESC’99, Vol. 2, pp. 947-952.

[4] Schulte, T., Fröhleke, N., and Grotstollen, H., “Control for Ultrasonic Motors with LLCC-Resonant Converter”, Proc. of Conf. on New Actuators 2000, Bremen, Germany, Juni, 2000, pp. 411-414.

[5] Njiende, H., Fröhleke, N., and Wallmeier, P., “Optimization of Inductors in Power Converters feeding High Power Piezoelectric Motors”, Proc. of AUPEC 2001 Conference, Perth, Sept. 2001.